Inhibition of apoptosis in breast cancer cells by si-FoxO3a through the protein digestion and absorption signaling pathway

LIYING SUN[1,2*], ZHONGXU WANG[1,3*], YANXI LIU[1], JIAXIN LV[1], XIAOTONG SHAO[1], HAOMING TANG[1], CHENG HU[1], LIANG CAO[1], YUNDONG ZHAO[4] and SHUANG CHEN[1,3]

[1]College of Laboratory Medicine, Jilin Medical University, Jilin, Jilin 132013, P.R. China; [2]Clinical Laboratory Center, Laboratory Department, Jilin Women and Children Health Hospital, Changchun, Jilin 130061, P.R. China; [3]Medical College, Translational Medicine Research Center, Dalian University, Dalian, Liaoning 116622, P.R. China; [4]College of Medical Technology, Beihua University, Jilin, Jilin 132013, P.R. China

Received January 24,2025; Accepted September 16, 2025

DOI: 10.3892/ol.2025.15345

Abstract. FoxO3a is closely associated with the occurrence and development of tumors. The present study aimed to evaluate the effect of FoxO3a on apoptosis in breast cancer, and to clarify the regulation of the protein digestion and absorption pathway in two breast cancer cell lines, through interfering with the expression of FoxO3a. MCF-7 and MDA-MB-231 were selected as the focal cells to study, and small interfering (si)RNA transfection technology was used to knockdown the expression of FoxO3a in both cell types. Clinical antitumor drugs were selected to treat cancer cells transfected with negative control sequences (si-NC) and sequences targeting FoxO3a (si-FoxO3a) in order to determine both the number of apoptotic cells and their morphology, and to assess migration levels using a wound healing assay. The cells were divided into si-NC and si-FoxO3a dosing groups for proteomics analyses, which were conducted using the differentially expressed proteins (DEPs) and the common signaling pathways were investigated. Finally, key proteins were validated using western blotting. First, the baseline expression levels of FoxO3a in two types of breast cancer cells were validated, confirming the presence of FoxO3a expression in both cell types. Next, FoxO3a was knocked down. Drug concentrations of tamoxifen (25 μmol/ml) and doxorubicin (30 μmol/ml) were selected for MCF-7 and MDA-MB-231 cells, respectively. si-FoxO3a reduced tumor cell death, and the apoptosis rate of cells treated with si-FoxO3a was notably decreased, indicated by Hoechst staining with reduced brightness. There was also a notable increase in scratch healing rate. After screening of DEPs by proteomics analysis, Gene Ontology enrichment analyses revealed common molecular functions of DEPs in both breast cancer cell lines at the cellular component and molecular function levels, predominantly extracellular space and L-glutamine transmembrane transporter activity. Kyoto Encyclopedia of Genes and Genomes functional enrichment analysis demonstrated that the main signaling pathway involved in apoptosis of both cell lines after FoxO3a knockdown was the protein digestion and absorption pathway. Protein-protein interaction mapping results showed a close relationship between DEPs. Focal DEPs were validated, and the findings were consistent with the proteomics results. Overall, the results demonstrated that si-FoxO3a inhibited the apoptosis of breast cancer cells through the protein digestion and absorption signaling pathway.

Correspondence to: Dr Shuang Chen, College of Laboratory Medicine, Jilin Medical University, 5 Jilin Street, Fengman, Jilin 132013, P.R. China
E-mail: 64109122@qq.com

*Contributed equally

Key words: breast cancer, apoptosis, proteomics, protein digestion and absorption signaling pathway, interference with FoxO3a

Introduction

Breast cancer is the most common malignant tumor in female patients (1); according to data from the World Health Organization, in 2020, there were ~2.26 million new breast cancer cases worldwide, threatening their lives by affecting both physical and psychological health (2,3). The latest advancements in treatment have mainly focused on the use of molecular biology and immunological approaches to develop highly targeted therapies for different types of breast cancer. This has been explored through inhibiting specific targets or molecules that promote tumor progression (4). Due to the presence of different subtypes and differences in treatment modalities (5), it is common to categorize breast cancers on the basis of expression patterns of three receptors: Estrogen receptor, progesterone receptor and human epidermal growth factor-2 (HER2) receptor, or as a triple-negative breast cancer (TNBC). Most patients suffer from estrogen receptor-positive breast cancers; the majority of patients have estrogen receptor-positive breast cancer, accounting for >70% of all cases (6), *in vitro* models are primarily represented by MCF-7 cells. Endocrine therapy, usually using tamoxifen (TAM), has been shown to markedly prolong the survival of patients with breast cancer (7). TNBC, a subtype in which estrogen, progesterone and HER2

receptors are not expressed, accounts for 12-17% of invasive breast cancers (8,9) and 83% of total mortalities (10). Compared with other breast cancer subtypes, triple-negative breast cancer (TNBC), represented by the MDA-MB-231 cell line *in vitro* , has the highest recurrence and metastasis rates and is exemplified by development at a young age and a poor prognosis (11). Currently, there are no effective treatments other than surgery, radiation and chemotherapy therapy. Doxorubicin (DOX) is widely used to treat TNBC (12), as a chemotherapy drug, therefore in the present study, both TAM and DOX were chosen to induce apoptosis in breast cancer cells.

Multiple transcription factors have been reported to regulate proliferation and apoptosis in breast cancer cells (13,14). These transcription factors achieve these effects by controlling protein translation and degradation. Consequently, interactions between proteins and transcription factors play a crucial role in the initiation and progression of breast cancer (15,16). The transcription factor FoxO3a has potent tumor suppressor effects in a variety of malignancies, such as gastric, prostate and colorectal cancers (17-19). RNA interference targeting FOXO3a was used to measure the impact of simvastatin on FOXO3a-expressing cells (20). Therefore, the present study performed FoxO3a knockdown. Previous studies have shown that low expression of FoxO3a could inhibit the apoptosis of tumor cells (21,22).

The application of proteomics allows for the discovery of additional proteins, which can provide insight into the mechanisms of disease and identify specific biomarkers that induce apoptosis. In the present study, small interfering (si)RNA-negative control (NC) and si-FoxO3a cel ls from two types of breast cancer were treated with TAM and DOX to construct estrogen-dependent and triple-negative si-FoxO3a breast cancer cell lines. The aims were to validate the effect on drug-induced apoptosis in breast cancer cells after interference with FoxO3a, analyze the signaling pathways that serve a role in the regulation of apoptosis after treatment via proteomics; and validate the signaling pathway-associated differentially expressed proteins (DEPs). The present study hypothesizes that targeting regulatory proteins in protein digestion and absorption signaling pathway could lead to timely detection of breast cancer metastasis and improve treatment outcomes.

Materials and methods

Cell culture. Breast epithelial cells, MCF-10A, and breast cancer cell lines MCF-7 and MDA-MB-231 were purchased from the Shanghai Institute of Biological Sciences. The cells were cultured in RPMI-1640 (Gibco; Thermo Fisher Scientific, Inc.) and high-glucose DMEM (both Gibco; Thermo Fisher Scientific, Inc.), supplemented with 10% FBS (EvaCell) and 1% penicillin and streptomycin (Cytiva) at 37˚C with 5% CO_2.

Cell transfection. A total of $2.5x10^5$ cells/well (MCF-7 and MDA-MB-231) were seeded into 6-well plates and incubated at 37˚C for 24 h. Liposomal transfection of siRNA was performed the following day when the cell density reached 60% using the transfection reagent Lipofectamine® 3000 (Thermo Fisher Scientific, Inc.) for 24 h at 37˚C. The siRNAs were designed by our laboratory staff and synthesized by Guangzhou Ruibo Biotechnology Co., Ltd. In addition, 1,750 ml basal medium, 5 μl siRNA, 5 μl transfection reagent and 240 μl serum-free medium was added to each well. At 8 h after transfection in serum-free medium, the medium was replaced with complete medium and the cells were incubated for a further 24 h. si-FoxO3a target sequence was 5'-AATGATGGGGGGCTG ACTGAAA-3', synthesized by RiboBio Biotechnology, the initial siRNA transfection concentration is 50 nmol.

Reverse transcription quantitative PCR (RT-qPCR). Total cellular RNA was extracted with TRIzol® reagent (Invitrogen; Thermo Fisher Scientific, Inc.) for reverse transcription (SureScript™ First-Strand cDNA; Thermo Fisher Scientific, Inc.). The quality and concentration of the extracted RNA was analyzed using spectrophotometry (NanoDrop Technologies; Thermo Fisher Scientific, Inc.). Reverse transcription conditions are as follows: 25˚C 5 min, 42˚C 15 min, 85˚C 5 min. Blaze Taq SYBR® Green qPCR Mix 2.0 (Thermo Fisher Scientific, Inc.) was used for RT-qPCR experiments. Thermocycling conditions: 95˚C pre-denaturation for 10 min, 95˚C denaturation for 15 sec, 60˚C annealing for 1 min, 72˚C extension for 30 sec, repeated for 40 cycles, with three replicate wells per sample, and the transcript levels were normalized to those of GAPDH. Gene expression levels were analyzed using the $2^{-\Delta\Delta Cq}$ method (23). The following primers were used: GAPDH-forward (F): 5'-ACCCACTCCTCCACC TTTGAC-3'; GAPDH-reverse (R): 5'-TGTTGCTGTAGC CAAATTCGTT-3'; FoxO3a-F: 5'-CGGACAAACGGCTCA CTCT-3'; FoxO3a-R: 5'-GGACCCGCATGAATCGACTAT-3';

Western blotting. Experiments were performed with MCF-7/MDA-MB-231 si-NC and si-FoxO3a cells treated with TAM/DOX for 24 h, which were both washed twice with PBS and lysed on ice for 30 min with the addition of lysis buffer(Beyotime Biotechnology). Centrifugation was performed at 12,000 x g for 10 min at 4˚C. The supernatant was collected, and the protein concentration was determined using the Enhanced BCA Protein Assay kit (Beyotime Institute of Biotechnology). A total of 5 μg/lane protein per well,, separated by SDS-PAGE (5% concentrating and 5% separating gel), transferred to a PVDF membrane and incubated overnight at 4˚C with the following primary antibodies: GAPDH (1:1,000; cat. no. P04406; Cell Signaling Technology, Inc.), FoxO3a (1:1,000; cat. no. O43524; Cell Signaling Technology, Inc.), trophoblast glycoprotein (TPBG; 1:1,000; cat. no. Q13641; Cell Signaling Technology, Inc.), sodium-coupled neutral amino acid symporter 2 (SLC38A2; 1:1,000; cat. no. DF4673; Affinity Biosciences), asparagine synthetase (ASNS; 1:1,000; cat. no. P08243; Cell Signaling Technology, Inc.), phosphorylated (p)-FOXO3a (1:1,000; cat. no. O43524; Cell Signaling Technology, Inc.) and zyxin (ZYX; 1:1,000; cat. no. Q15942; Cell Signaling Technology, Inc.). The membrane was washed three times, incubated with a goat anti-rabbit IgG antibody (1:1,000; cat. no. 210830803; Beijing Zhongshan Jinqiao Biotechnology Co., Ltd.) for 1 h at room temperature, and the results were detected with a chemiluminescent ECL detection system(Thermo Fisher). The experiments all contained three independent biological replicates, and three technical replicates were used for each biological replicate to ensure data reliability.

Water-soluble tetrazolium salt (WST-1) assay. A total of $6x10^3$ cells per well were seeded in a 96-well plate, and three

replicate wells were used for each group. When the density reached 80-90%, the culture medium was discarded, and 100 μl different concentrations of TAM/DOX were added. Each well had 10 μl WST-1 reagent added 24 h after the drug treatment, the reaction was carried out at 37˚C for 15-30 min and the optical density value was assessed at the wavelength of 460 nm. The experiments all contained three independent biological replicates, and three technical replicates were used for each biological replicate to ensure data reliability.

Cell apoptosis. A total of 2.5x10^5 cells were seeded in a 6-well plate and digested with trypsin. Following centrifugation for 10 min at 4˚C, 12,000 x g the cells were resuspended in PBS, centrifuged again and then, according to the protocol of the FITC-coupled Annexin-V Apoptosis Detection Kit (BD Biosciences), each sample was mixed with 490 μl 1X binding buffer and 5 μl each of FITC and PI dyes. The cells were stained for 20 min at room temperature, protected from light and assessed using flow cytometry within 1 h. There were 10,000 cells in each group. The experiments all contained three independent biological replicates, and three technical replicates were used for each biological replicate to ensure data reliability.

Hoechst staining. Hoechst 33342 is a dye that penetrates cell membranes, causing living cells to fluoresce blue. When apoptosis occurs with inconsistent nuclear fragmentation; the brightness of the blue fluorescence is increased. A total of 10,000 si-NC and si-FoxO3a cells were cultured for 6-8 h, the cells were treated with the drugs for 24 h, the supernatant was discarded and the cells were washed twice with precooled PBS. Hoechst 33342 staining solution (Thermo Fisher Scientific, Inc.) was added, and the cells were stained for 15-20 min at room temperature, before being washed three times with precooled PBS at 4˚C for 5 min each. The fluorescent intensity of the cells was observed using fluorescence microscopy. The experiments all contained three independent biological replicates, and three technical replicates were used for each biological replicate to ensure data reliability.

Wound healing assay. MCF-7 and MDA-MB-231 cells were seeded into 6-well plates (3x10^5 and 5x10^5/well, respectively), and the transfection and drug treatments were carried out as aforementioned. After the cells grew to 90% confluence, a sterile tip was used to scratch the cells. Cell debris was removed by washing with PBS and the cells were cultured in serum-free medium for 24 h. Images were acquired using a fluorescence microscope (magnification, x10) at 0 and 24 h after scratching. The relative size of the wound area from 0 to 24 h was measured using Image J software(National Institutes of Health; version no. 1.47) to calculate the cell migration rate. The experiments all contained three independent biological replicates, and three technical replicates were used for each biological replicate to ensure data reliability.

Proteomics processing. MCF-7 and MDA-MB-231 cells treated with TAM/DOX drugs for 24 h were recorded as control (ctrl)-TAM and ctrl-DOX, respectively. FoxO3a knockdown cells treated with drugs for 24 h were recorded as si-TAM and si-DOX. After treatment, the cell precipitate was collected, 20% trichloroacetic acid was added, the mixture was vortexed well and the cells were left to precipitate for 2 h at 4˚C. The supernatant was removed by centrifugation at 4˚C, 4,500 x g for 5 min, and the precipitate was washed with precooled acetone 2-3 times. The precipitate was allowed to dry, a final concentration of 200 mM triethylammonium bicarbonate was added, the precipitate was broken by ultrasonication and it was enzymatically digested overnight. Dithiothreitol was added to a final concentration of 5 mM and reduced at 56˚C for 30 min. Iodine-acetyl carbamate was added to a final concentration of 11 mM and incubated for 15 min at room temperature in the dark. The confidence interval for the difference in the protein quantification ratio between the si-FoxO3a and the si-NC group was assessed as the multiplicity of differences, with a fold-change >1.2 and P<0.05. The false discovery rate (FDR) for protein identification and peptide-spectrum match identification in the search database settings was 1%, revealing that different protein networks existed in both cancer cell lines after interfering with FoxO3a expression.

Liquid chromatography-mass spectrometry analysis. Liquid chromatography-mass spectrometry analysis was performed by Jingjie PTM Bio-Laboratory (Hangzhou) Co., Ltd. using positive ionization mode. The primary mass spectrometry scan range was 400-1,200 m/z with a resolution of 60,000. The fixed starting point for the secondary mass spectrometry scan range was 110 m/z, with a secondary scan resolution of 15,000. Mobile phase A was an aqueous solution containing 0.1% formic acid and 2% acetonitrile; mobile phase B was an aqueous solution containing 0.1% formic acid and 90% acetonitrile. The liquid chromatography gradient settings were as follows: 0-68 min, 6-23%B; 68-82 min: 23-32%B; 82-86 min: 32-80%B; 86-90 min: 80%B. Flow rate maintained constant at 500 nl/min.

Gene Ontology (GO), KEGG(Kyoto Encyclopedia of Genes and Genomes) functional enrichment analysis, and STRING protein interactions. GO (geneontology.org) and KEGG (kegg.jp) functional enrichment analyses were performed based on secondary categorization and Fisher's exact test was applied to calculate the significance P-value with the aim of determining whether DEPs were significantly enriched in certain functional types. The FDR value in enrichment analysis is set to 1%. Directly copy or import the identified differentially expressed proteins into the STRING database (cn.string-db.org).

Statistical analyses. A Student's t-test (unpaired)was used to compare differences between two groups, and a one-way ANOVA followed by Tukey's post hoc test was used to compare differences between multiple groups. Calculations were performed using SPSS Statistics 17.0 (IBM Corp.) software, with normality analysis being performed using the Kolmogorov-Smirnov test. Three replications were performed for all the experiments, and the data are expressed as the mean ± standard deviation. P<0.05 was considered to indicate a statistically significant difference.

Results

Assessment of baseline expression levels of FoxO3a and successful knockdown of FoxO3a. FoxO3a expression was

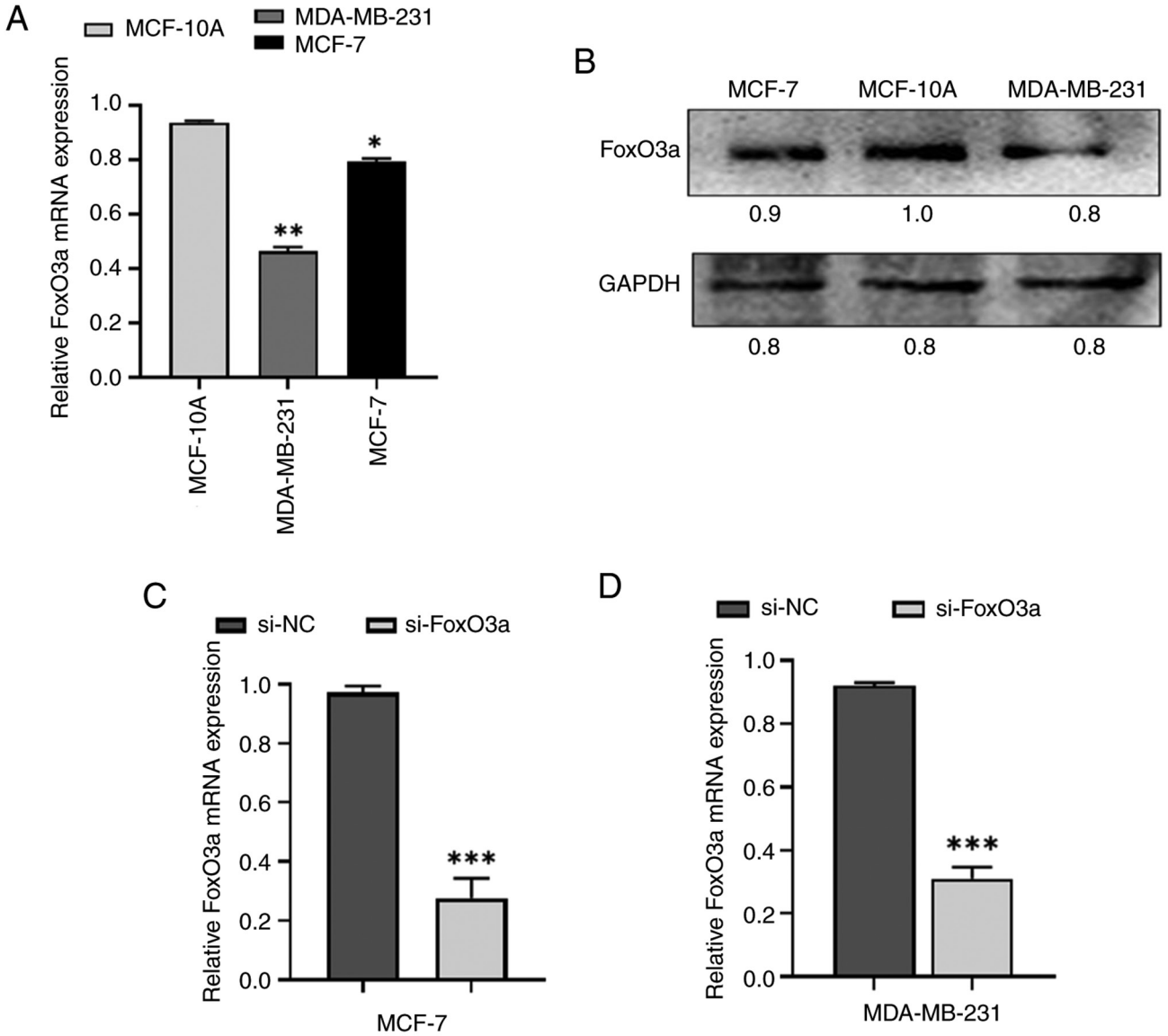

Figure 1. FoxO3a baseline level and efficiency of interference. (A) RT-qPCR detection of MCF-7 and MDA-MB-231 FoxO3a expression, and comparison with MCF-10A cells. (B) Western blot detection of MCF-7 and MDA-MB-231 FoxO3a expression, and comparison with MCF-10A cells. (C) RT-qPCR detection of FoxO3a expression level in MCF-7 cells. (D) RT-qPCR detection of FoxO3a expression level in MDA-MB-231 cells. *P<0.05; **P<0.01; ***P<0.001. RT-qPCR, reverse transcription quantitative PCR; si, small interfering RNA; NC, negative control.

examined in MCF-7 and MDA-MB-231 cells using RT-qPCR and western blotting, which demonstrated that FoxO3a levels were detected in both cell types (Fig. 1A and B). FoxO3a was successfully knocked down by transfection of siRNA for 24 h. RT-qPCR was used to assess the knockdown efficiency as shown in Fig. 1C and D.

si-FoxO3a decreases the degree of apoptosis

Annexin V/PI double staining demonstrates that si-FoxO3a hinders the apoptosis of breast cancer cells by antitumor drugs. The WST-1 assay was used to determine the optimal concentrations of TAM and DOX. This method is easy to perform, produces stable results and has low cytotoxicity. The results of the WST-1 assay revealed that the apoptosis rate of si-FoxO3a MCF-7 and MDA-MB-231 cells by 25 μmol/ml and 30 μmol/ml TAM and DOX respectively, was decreased compared with the si-NC cells (Fig. 2A and B). Flow cytometry was used to analyze the proapoptotic effects of 0 and 25 μmol/ml TAM drug treatments for 24 h on si-NC and si-FoxO3a MCF-7 cells, and 0 and 30 μmol/ml DOX drug treatments for 24 h on si-NC and si-FoxO3a MDA-MB-231 cells. The results (Fig. 2C and D) revealed that the apoptosis rates of the si-NC and si-FoxO3a MCF-7 cells were 8.95±0.04% and 7.81±1.17%, respectively, and the apoptotic rates of si-NC and si-FoxO3a MDA-MB-231 cells were 11.56±2.22% and 8.31±0.20%, respectively, when cultured for 24 h without treatment. The differences were not found to be statistically significant. These findings indicate that the transfection of siRNA had no significant effect on the level of apoptosis in either type of breast cancer cells. By contrast, when treated with drugs for 24 h, the apoptosis rates of the si-NC and si-FoxO3a treated MCF-7 cells were 21.22±0.88% and 10.10±0.44%, respectively, and the apoptosis rates of si-NC and si-FoxO3a MDA-MB-231 cells were 24.19±0.60% and 13.67±0.35%, respectively. The level

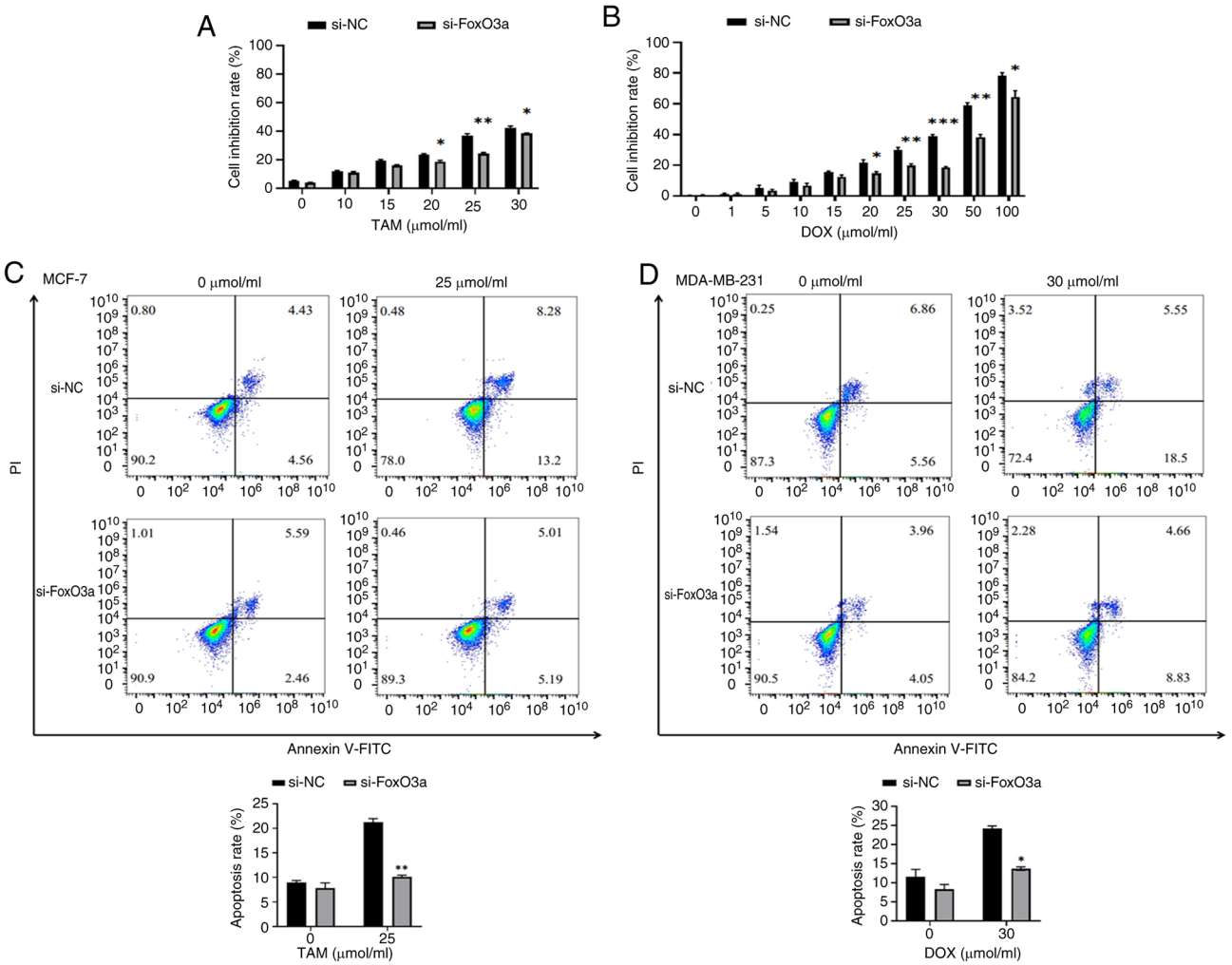

Figure 2. Water-soluble tetrazolium salt results and inhibitory effects of drugs on apoptosis of si-NC and si-FoxO3a cells. (A) Inhibitory effect of different concentrations of TAM on MCF-7 cells. (B) Inhibitory effect of different concentrations of DOX on MDA-MB-231 cells. (C) Flow cytometry analysis of the apoptosis rate of TAM (0 μmol/ml, 25 μmol/ml) treated MCF-7 si-NC and si-FoxO3a cells and results of the data analysis of apoptosis rate. (D) Flow cytometry analysis of the apoptosis rate of DOX (0 μmol/ml, 30 μmol/ml) treated MDA-MB-231 si-NC and si-FoxO3a cells and results of the data analysis of apoptosis rate. *P<0.05; **P<0.01; ***P<0.001. n=3, data shown as mean ± standard deviation. si, small interfering RNA; NC, negative control; TAM, tamoxifen; DOX, doxorubicin; PI, propidium iodine.

of apoptosis in si-FoxO3a cells was significantly reduced after treatment with the drug, demonstrating that interfering with FoxO3a decreases the sensitivity of cancer cells to the drug.

Hoechst staining demonstrates that si-FoxO3a hinders the inhibitory effect of antitumor drugs on breast cancer cells. si-NC cells and si-FoxO3a cells without drug treatment presented with dark blue fluorescence staining of the nuclei. After drug treatment for 24 h, the nuclear staining of the two types of breast cancer cells was not homogeneous, as there was some nuclear fragmentation, indicated by increased fluorescence brightness. Furthermore, the levels of nuclear fragmentation in si-FoxO3a cells were significantly reduced compared with si-NC cells. This indicates reduced apoptosis of si-FoxO3a cells. Quantification of the nuclear fragmentation levels is presented in Fig. 3A and B.

Wound healing assay demonstrates enhanced migration of si-FoxO3a cells. Subsequently, the migration of MCF-7 and MDA-MB-231 si-NC and si-FoxO3a cells towards the scratched area was observed. Without drug treatment, there was no significant difference in migration rates between si-NC and si-FoxO3a cancer cells. Following 24 h treatment with TAM and DOX, respectively, the migration rate of si-FoxO3a cells was significantly increased compared to the si-NC group (Fig. 4A and B). This indicates that FoxO3a knockdown reduces cancer cell death and enhances their migratory capacity.

Proteomics analysis of DEPs in si-FoxO3a. The study consisted of si-FoxO3a and si-NC groups for label-free quantitative proteomics analysis, with three biological replicates for each group. A screen for DEPs by the ratio of quantitative values of DEPs in si-FoxO3a to si-NC cells revealed 206 DEPs in MCF-7 and 207 DEPs in MDA-MB-231 cells, with 15 proteins in crossover and subcellular localization analysis. The volcano plots (Fig. 3C and D) show that TPBG, SLC38A2, ATP binding cassette subfamily D member 1, endothelin converting enzyme 1, ASNS, ferritin heavy chain 1 (FTH1), ZYX, stomatin, solute carrier family 2 member 1 (SLC2A1), serpin family B member 5, prothymosin α, phosphoglycerate dehydrogenase, methylenetetrahydrofolate dehydrogenase

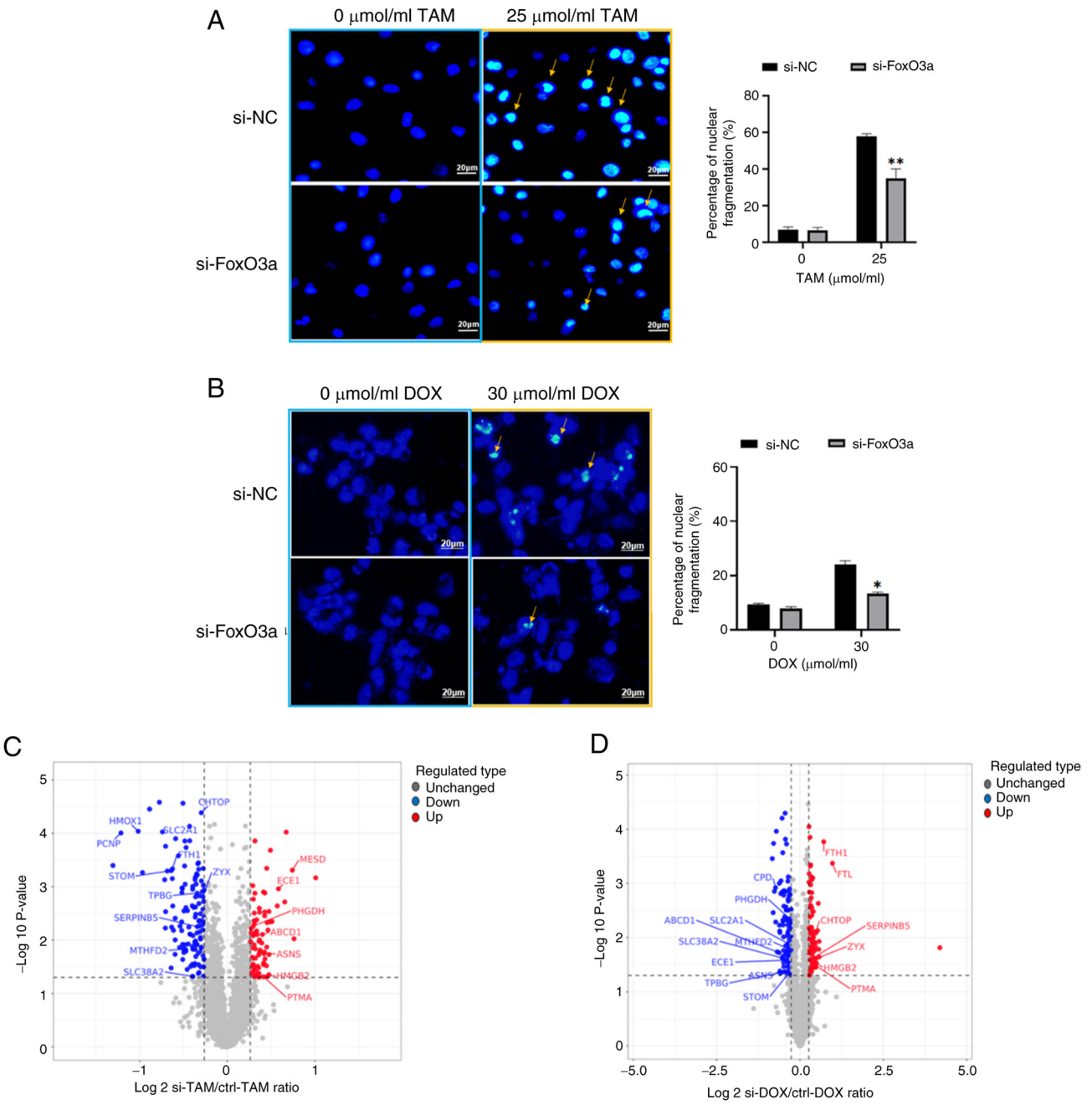

Figure 3. Hoechst staining results of si-NC and si-FoxO3a cells after drug treatment and volcano plot of differentially expressed proteins. (A) MCF-7 si-NC and si-FoxO3a cells without TAM treatment had no obvious apoptotic morphology. Cells in both groups showed apoptotic morphology after TAM treatment. Magnification, x400. (B) MDA-MB-231 si-NC and si-FoxO3a cells without DOX treatment had no obvious apoptotic morphology. Cells in both groups showed apoptotic morphology after DOX treatment. Magnification, x400. (C) Significantly downregulated proteins of MCF-7 cells are shown on the left side of the vertical dashed line. Significantly upregulated proteins are shown on the right side of the vertical dashed line. Non-significantly altered proteins are shown in gray. (D) Significantly downregulated proteins of MDA-MB-231 cells are shown on the left side of the vertical dashed line. Significantly upregulated proteins are shown on the right side of the vertical dashed line. Non-significantly altered proteins are shown in gray. n=3, data shown as mean ± standard deviation. *P<0.05; **P<0.01. si, small interfering RNA; NC, negative control; TAM, tamoxifen; DOX, doxorubicin; ctrl, control.

(NADP^{+} dependent) 2, high mobility group box 2 and chromatin target of PRMT1 (CHTOP) were DEPs common to the two types of cells after knockdown of FoxO3a. The presence of coregulatory proteins could provide new perspectives on the treatment and mitigation of drug resistance in both types of breast cancer.

Subcellular localization analysis. Subcellular localization analysis was performed on the identified DEPs. DEPs in MCF-7 cells were located mainly in the nucleus (n=63), cytoplasm (n=55) and plasma membrane (n=24). DEPs in MDA-MB-231 cells were located predominantly in the nucleus (n=49), cytoplasm (n=47) and plasma membrane (n=34). Therefore, the nucleus and cytoplasm are the regions where DEPs are predominantly localized in these two types of breast cancer cells (Fig. 5A and B). This is a major region of protein synthesis and energy transfer, therefore alterations of proteins within this region can affect the structure and

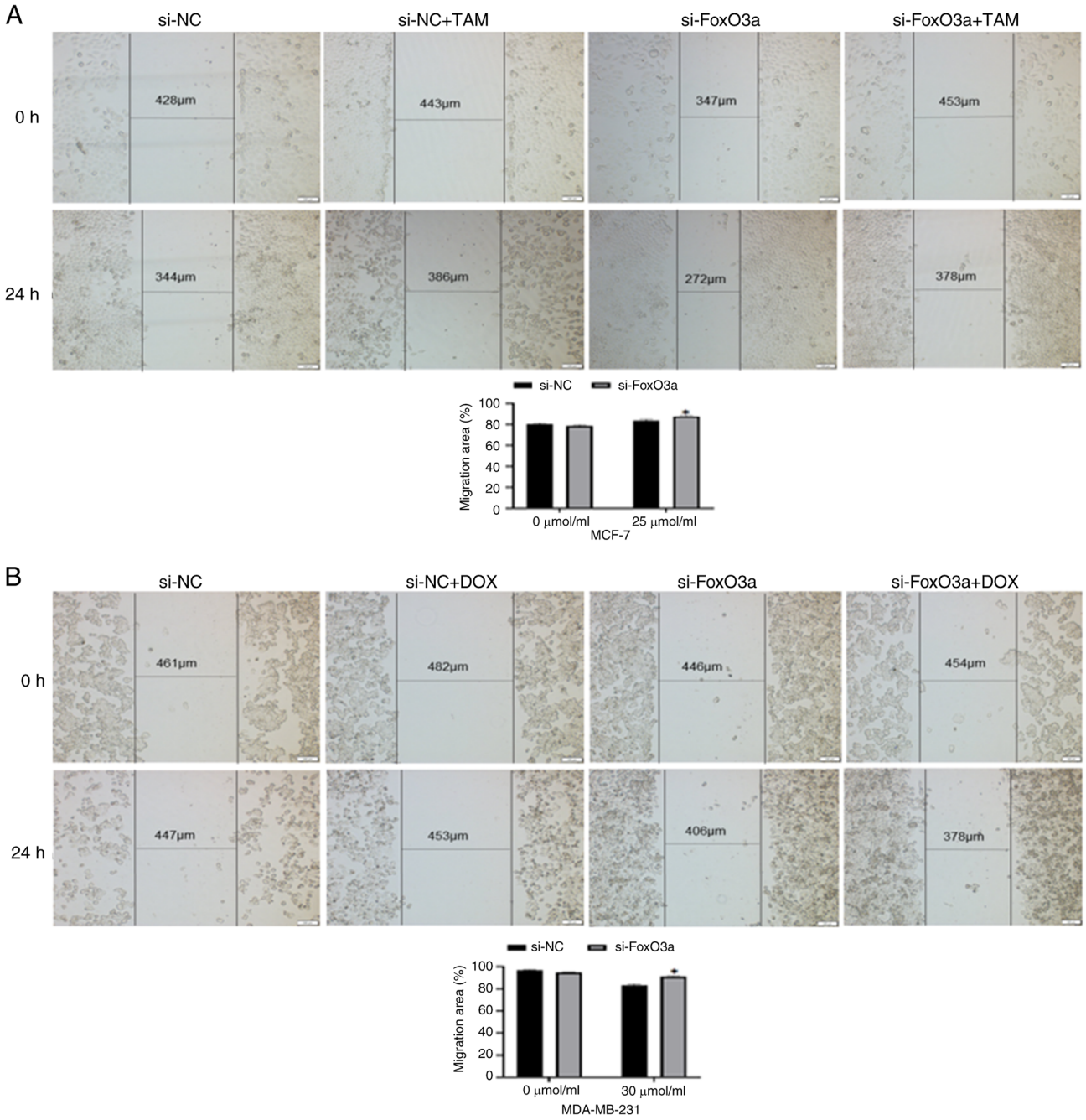

Figure 4. Migration of si-NC and si-FoxO3a cells after drug treatment. (A) Effect of TAM (0 μmol/ml, 25 μmol/ml) treatment on the migratory ability of MCF-7 si-NC and si-FoxO3a cells. (B) Effect of DOX (0 μmol/ml, 30 μmol/ml) treatment on the migratory ability of MDA-MB-231 si-NC and si-FoxO3a cells. *P<0.05. si, small interfering RNA; NC, negative control; TAM, tamoxifen; DOX, doxorubicin.

biological function of other relevant proteins and thus regulate breast cancer progression.

Gene Ontology (GO) secondary classification map. The GO database (geneontology.org) is designed to qualify and characterize gene and protein functions in three categories: Biological process (BP), molecular function (MF) and cellular component (CC). The y-axis represents the GO classification, and the x-axis represents the number of proteins. Fig. 6A and B shows the involvement of >100 differentially expressed upregulated and downregulated proteins in each of the three major classifications of the GO database. The DEPs of the two breast cancer cell lines coregulate BP processes such as 'cellular process', 'biological regulation', 'metabolic process', 'response to stimulus' and 'multicellular organismal processes'. These proteins are primarily localized to the 'intracellular anatomical structure' and perform the MF of 'binding' (Fig. 6A and B).

KEGG secondary classification map. As shown in Fig. 5, MCF-7 and MDA-MB-231 cellular DEPs share common BPs and functions across multiple KEGG secondary classifications. Most of these DEPs were involved in the CP of 'transport and catabolism' and 'cell growth and death'; 'signal transduction' in EIP, suggesting a close relationship with signaling pathways; 'translation' and 'folding, sorting and degradation' in GIP,

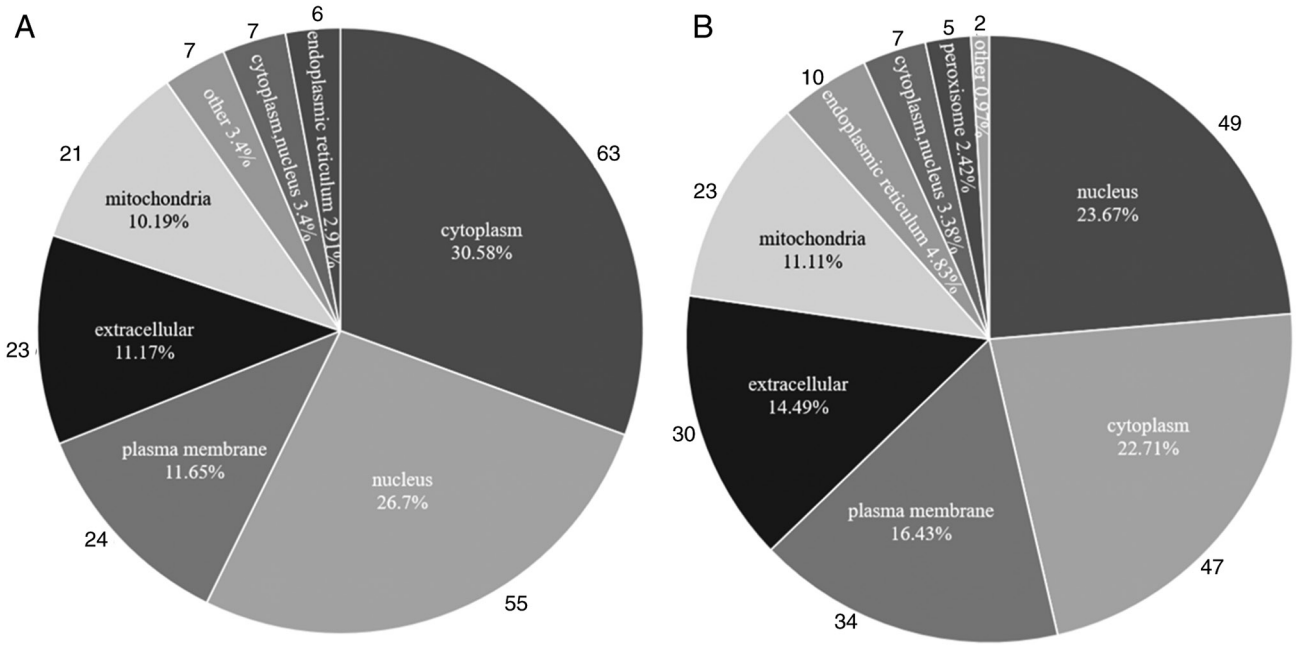

Figure 5. Pie charts of subcellular localization. (A) Pie chart of subcellular localization of differentially expressed proteins in MCF-7 cells. (B) Pie chart of subcellular localization of differentially expressed proteins in MDA-MB-231 cells.

suggesting an association with protein structure and function; 'infectious disease: viral' and 'cancer: overview' in HD; 'global and overview maps' in metabolism; and the 'endocrine system' and 'digestive system' in OS (Fig. 7A and B). The description involved the process of protein digestion and absorption.

GO and KEGG pathway enrichment analysis. To understand the functions of the DEPs, the GO database was used to classify the enrichment of the screened DEPs. The DEPs identified in MCF-7 cells were enriched mainly at the BP level in 'ribosome biogenesis' and 'protein localization to the membrane'. The BP process of DEPs identified in MDA-MB-231 cells was enriched mainly in the 'cell surface receptor signaling pathway' and 'regulation of the defense response'. Notably, the common molecular functions of DEPs in both breast cancer cell lines at the CC and MF levels, are mainly seen in the 'extracellular space' and 'L-glutamine transmembrane transporter activity' (Fig. 8A-D). This suggests that there are similar signaling pathway functions of the DEPs of two si-FoxO3a breast cancer cell types and they are associated with amino acid transport.

The results of KEGG enrichment analysis demonstrated that DEPs in two si-FoxO3a breast cancer cell lines after treatment with two drugs were enriched mainly in the 'map04974 protein digestion and absorption' and 'map04978 mineral absorption' signaling pathways (Fig. 9A and B). Considering the notable role that protein levels serve in the development of breast cancer, and the combined subcellular localization analysis and GO enrichment results, primarily targeting the activity of 'L-glutamine transmembrane transporter activity', demonstrated the role of transport proteins, the present study focused on the preceding signaling pathway (map04974).

FoxO3a regulates protein digestion and absorption signaling pathway-related proteins. Protein-protein interaction (PPI) network mapping was performed for common DEPs and DEPs involved in apoptotic processes, together with FoxO3a, in two types of breast cancer cells. The findings indicated that the DEPs are closely related to each other and are involved in the regulation of protein digestion and absorption signaling pathways and apoptotic processes. -Therefore, DEPs identified in MCF-7 and MDA-MB-231 cells involved in the protein digestion and absorption signaling pathway and apoptosis, were mapped together with FoxO3a. This was performed using the STRING database to identify potential relationships between the proteins (Fig. 9C).

Western blotting for verification of the DEPs. The DEPs identified in the two types of breast cancer cells were validated using western blotting, which revealed that TPBG were downregulated and that p-FoxO3a levels were increased in si-FoxO3a cells compared with si-NC cells. ASNS was upregulated in MCF-7 cells and downregulated in MDA-MB-231 cells treated with si-FoxO3a. In addition, ZYX was upregulated in MCF-7 cells, and downregulated in MDA-MB-231 cells. The validation results were consistent with the proteomics results (Fig. 9D and E).

Discussion

Breast cancer, a malignant tumor with a high incidence and mortality rate, is a serious threat to women's lives and health (24). Drug resistance, recurrence and metastasis affect its treatment and prognosis. Thus, the search for reliable molecular markers can aid in the implementation of targeted therapy strategies for breast cancer, to overcome resistance to existing chemotherapeutic agents. The estrogen receptor antagonist TAM can be used as a first-line therapeutic agent as ~70% of breast cancers are estrogen receptor-positive. DOX is one of the most active agents against metastatic breast cancer cells, especially TNBC, and targeting tumor cells by loading

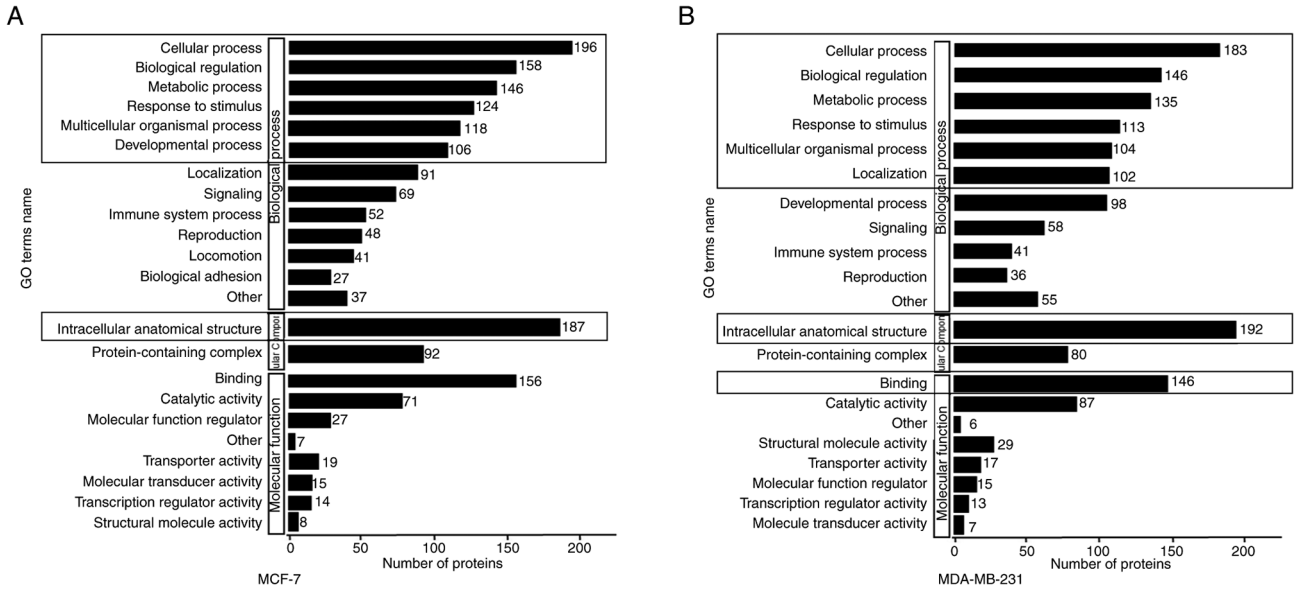

Figure 6. GO secondary classification chart. (A) GO secondary classification bar chart of MCF-7 cells. (B) GO secondary classification bar chart of MDA-MB-231. GO, gene ontology.

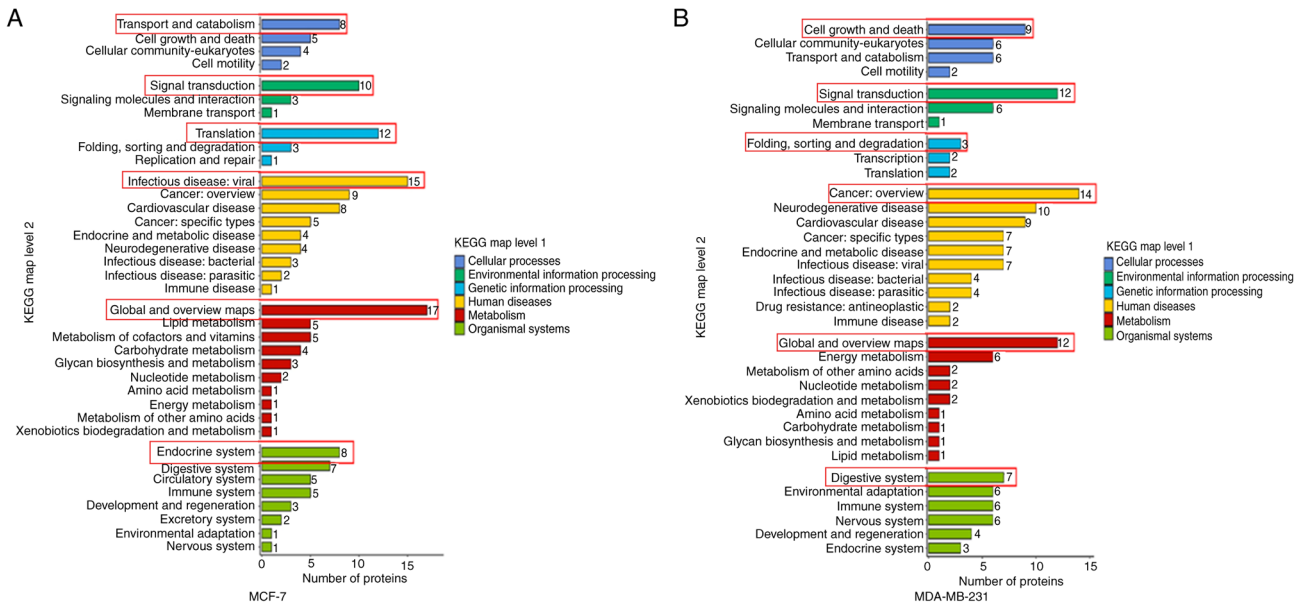

Figure 7. KEGG secondary classification chart. (A) Boxed out KEGG classification map representing the majority of differentially expressed proteins in MCF-7 cells. (B) Boxed out KEGG classification map representing the majority of differentially expressed proteins in MDA-MB-231 cells. KEGG, Kyoto Encyclopedia of Genes and Genomes.

DOX-carrying liposomes onto the surface of macrophages can enhance antitumor immune responses (25). Some side effects are associated with prolonged drug use, and numerous efforts have been made by researchers to mitigate these effects and improve their efficacy (26). Existing studies have demonstrated that the sirtuin 1/AKT pathway can overcome DOX treatment resistance (27). Exploring signaling pathways may be an effective approach to improving drug efficacy. FoxO3a has gradually attracted the attention of researchers as a transcription factor that has tumor suppressor potential and is involved in multiple signaling pathways. We have previously demonstrated its notable regulatory role in a variety of malignant tumors (28), mainly involving regulating BPs such as apoptosis, autophagy, DNA damage repair and angiogenesis to influence tumor progression (29-31). Our previous experiments revealed that FoxO3a can be altered during drug-induced autophagy in MCF-7 cells (21). Therefore, the present study analyzed the changes in signaling pathway proteins that occur when TAM and DOX cause apoptosis in cancer cells. This was performed using proteomic analysis of si-FoxO3a treated cells to identify the metastatic process and provide a scientific basis for overcoming therapeutic resistance.

FoxO3a expression was assessed in two breast cancer cell lines before being successfully knocked down and evaluated

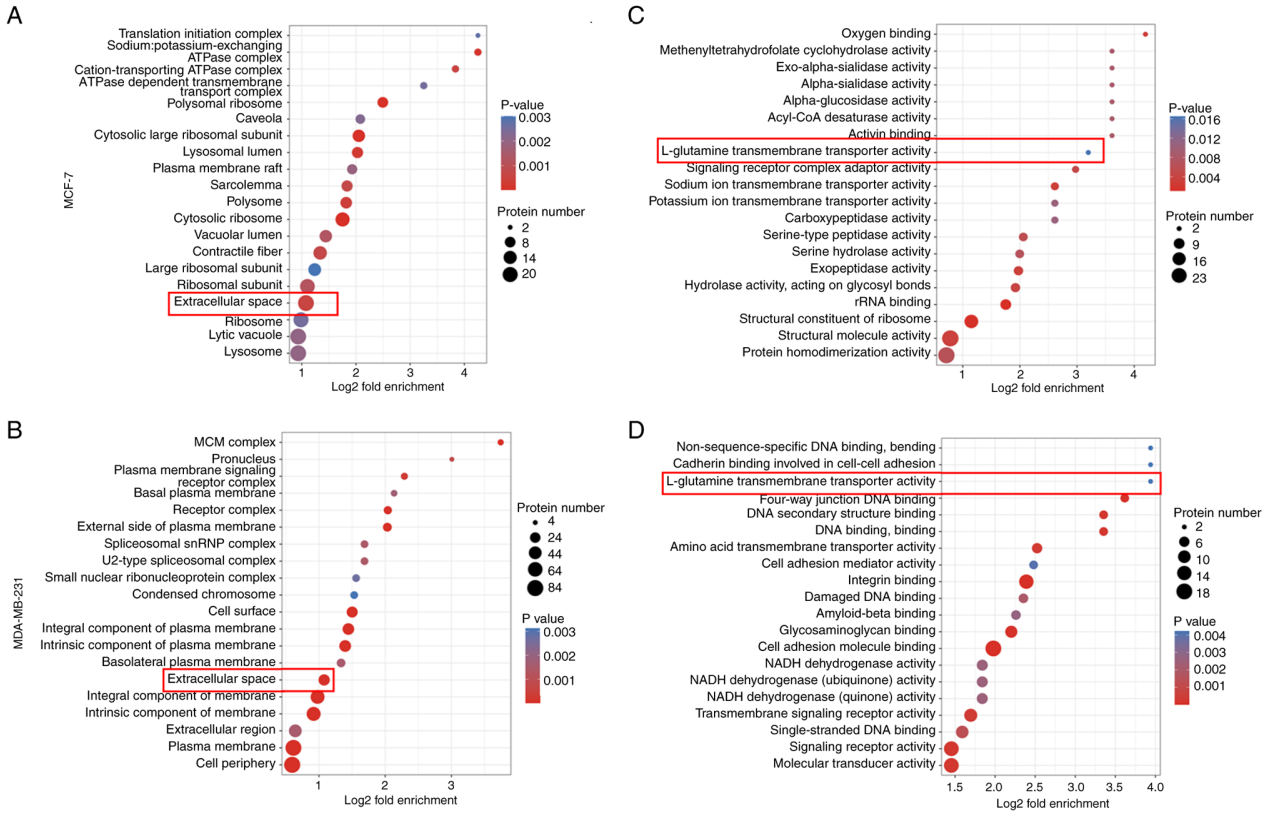

Figure 8. GO enrichment analysis bubble plots of DEPs. (A) Bubble plot of MCF-7 cells DEPs at the CC level of GO enrichment analysis. (B) Bubble plot of MDA-MB-231 cells DEPs at the CC level of GO enrichment analysis. (C) Bubble plot of MCF-7 cells DEPs at the MF level of GO enrichment analysis. (D) Bubble plot of MDA-MB-231 cells DEPs at the MF level of GO enrichment analysis. GO, gene ontology; DEPs, differentially expressed proteins; CC, cellular component; MF, molecular function.

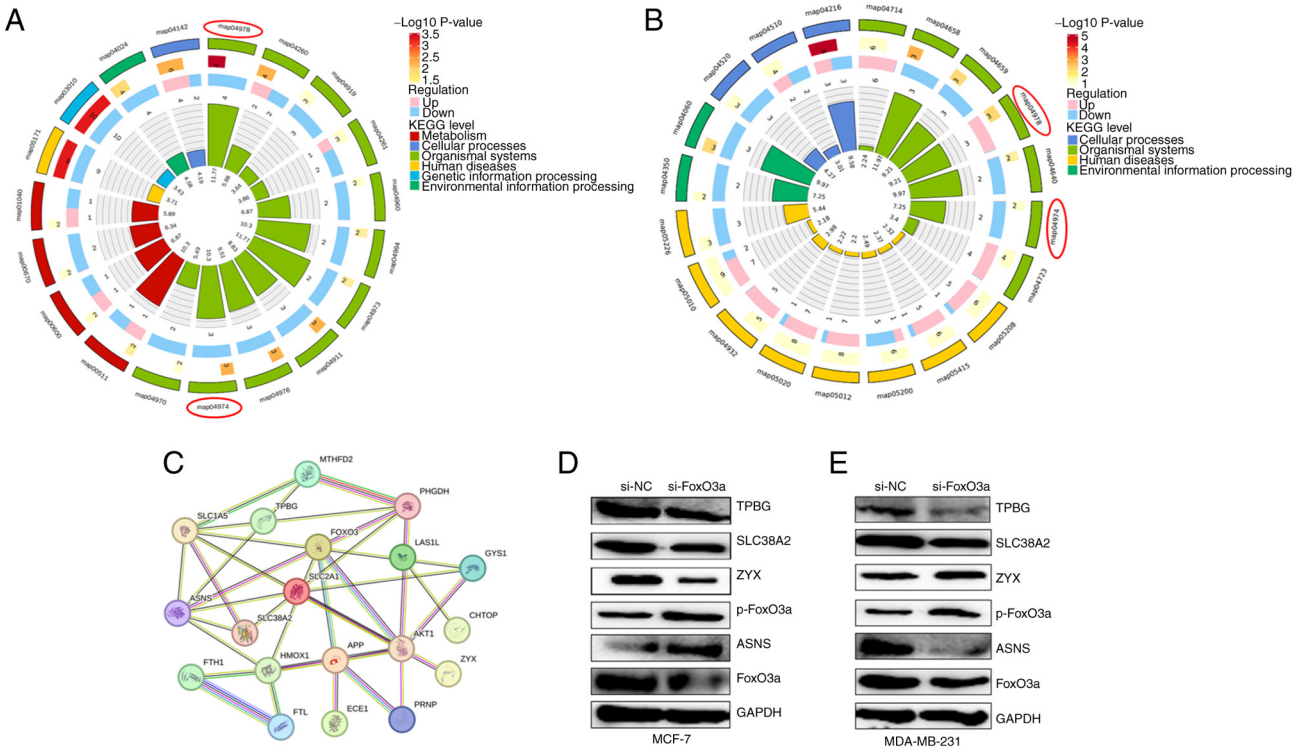

Figure 9. Circos plot of DEPs KEGG pathway enrichment, interaction diagram of DEPs with FoxO3a and western blot results. (A) Circos plot of MCF-7 cell DEPs. (B) Circos plot of MDA-MB-231 cell DEPs. map04974 represents the protein digestion and absorption signal pathway. (C) Protein-protein interaction diagram of DEPs with FoxO3a. (D) The expression of DEPs in MCF-7 cells was assessed using western blotting. (E) The expression of DEPs in MDA-MB-231 cells was verified using western blotting. DEP, differentially expressed protein; KEGG, Kyoto Encyclopedia of Genes and Genomes; si, small interfering RNA; NC, negative control; TPBG, trophoblastic glycoprotein; SLC38A2, solute carrier family 38 member 2; ZYX, zyxin; ASNS, asparagine synthetase.

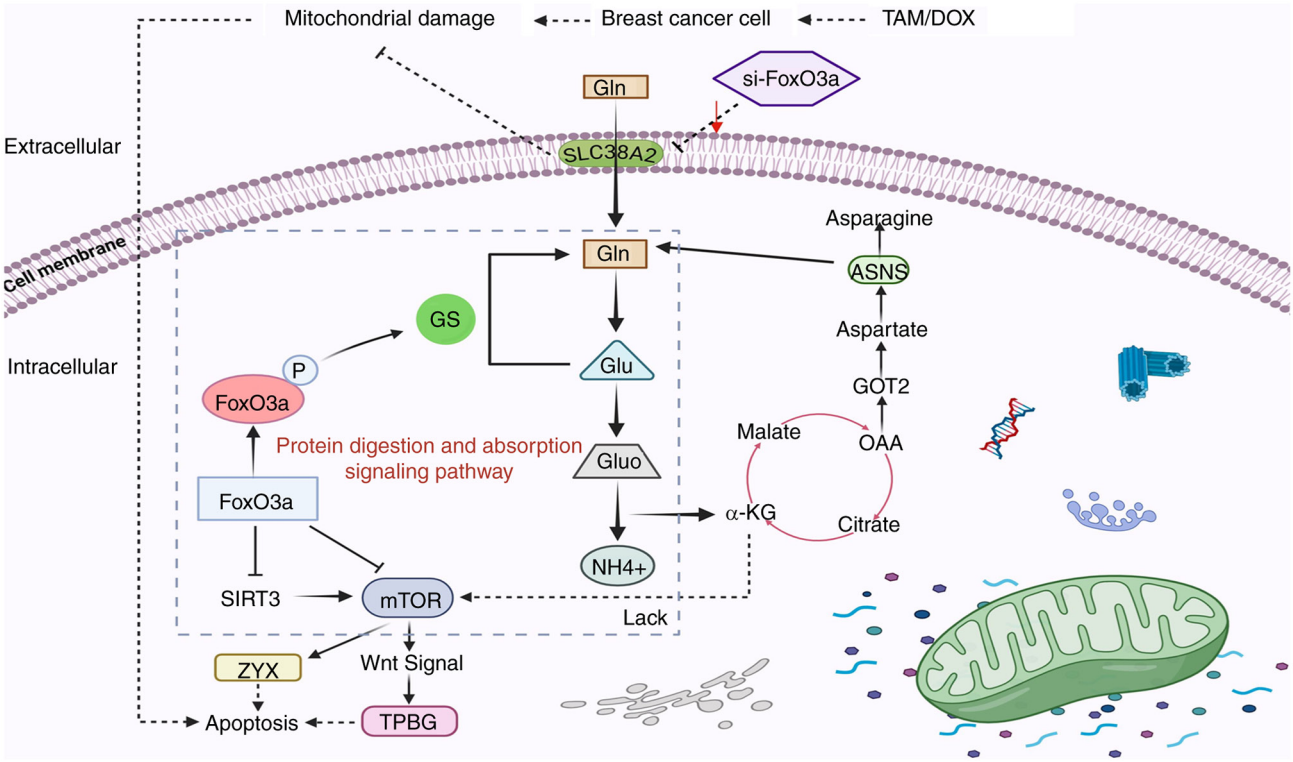

Figure 10. FoxO3a regulates the protein digestion and absorption signaling pathway. Antitumor drugs act on breast cancer cells, inducing mitochondrial damage and triggering the internal apoptotic program of cancer cells. si-FoxO3a impedes the mitochondrial damage process and affects Gln transport into the cell by decreasing the expression of the amino acid transport protein SLC38A2. This leads to a decrease in the conversion of Gln to glutamate, a decrease in the tricarboxylic acid cycle intermediate product OAA and the catalytic function of ASNS cannot be effectively performed. α-KG deficiency decreases mTOR expression. FoxO3a suppresses mTOR expression, thereby inhibiting ZYX expression and promoting cancer cell apoptosis. FoxO3 also affects TPBG levels through regulation of the Wnt signaling pathway to promote apoptosis in cancer cells. si, small interfering; SLC38A2, solute carrier family 38 member 2; ASNS, asparagine synthetase; α-KG, α-ketoglutarate; mTOR, mechanistic target of rapamycin kinase; TPBG, trophoblastic glycoprotein; ZYX, zyxin; Gluo, glutamate dehydrogenase; OAA, oxaloacetic acid; GS, glutamine synthetase.

using RT-qPCR. Control and FoxO3a knockdown cell models of estrogen-dependent MCF-7 cells and triple-negative MDA-MB-231 cells, were denoted as si-NC and si-FoxO3a, respectively. The concentrations of 25 and 30 μmol/ml for TAM and DOX, respectively, were determined using a WST-1 assay. The results demonstrated that si-FoxO3a cells were more resistant to drug-induced apoptosis in breast cancer cells compared with the si-NC cells, suggesting that interference with FoxO3a can reduce cancer cell death and increase their migration rate. The upper right quadrant of the flow cytometry results may reflect a mixture of late apoptotic cells and necrotic cells. Therefore, the present study further verified the level of apoptosis using Hoechst staining, indicating the FoxO3a transcription factor promotes drug-induced apoptosis in breast cancer cells. This should be validated using FoxO3a overexpression vectors in the future.

A study by Li *et al* (32) demonstrated that FoxO3a can be used as a potential therapeutic target for breast cancer; therefore, the development of FoxO3a-targeted drugs shows promise. Most of the DEPs were localized in the nucleus and cytoplasm regions, which are also the main regions for protein synthesis and energy transfer. GO enrichment analysis revealed common molecular functions of DEPs in both breast cancer cell lines at the CC and MF levels, mainly the extracellular space and L-glutamine (Gln) transmembrane transporter activity. These findings suggest that the DEPs are involved in the same signaling pathways of both si-FoxO3a breast cancer cell lines and are related to amino acid transport. This suggests modulating associated signaling pathway proteins by knocking down FoxO3a may be a key mechanism for drug-induced apoptosis in breast cancer cells. KEGG enrichment analysis indicated that the two si-FoxO3a breast cancer cell lines inhibited drug-induced apoptosis through the protein digestion and absorption signaling pathway. DEPs were selected to map the PPI network together with FoxO3a, and the connections between the protein and FoxO3a were assessed. The regulation of apoptosis in breast cancer cells following knock down of FoxO3a expression may involve other or parallel pathways. As indicated by GO and KEGG secondary classifications, differentially expressed proteins in the two breast cancer cell lines jointly regulate processes such as 'biological regulation', 'metabolic processes', and 'stimulus response'. Additionally, they are involved in 'translation' and 'folding, sorting, and degradation' in GIP. These processes are largely unrelated to mineral absorption, strongly suggesting an association with protein digestion and absorption functions. Therefore, the validation of proteins related to the protein digestion and absorption signaling pathway was primarily focused on. DEPs TPBG, SLC38A2, ASNS, ZYX and p-FoxO3a were selected for subsequent validation using western blotting, which yielded results consistent with those of the proteomic analysis. After FoxO3a is phosphorylated by kinases such as AKT, it is translocated from the cell nucleus, leading to loss of activity and reduced expression. At this point,

p-FoxO3a levels increase, and the AKT signaling pathway is generally activated. After FoxO3a is phosphorylated by kinases such as AKT, it translocated from the cell nucleus, leading to loss of activity and reduced expression.

The end products of protein digestion are amino acids, as seen in the cellular pathway diagram (Fig. 10) and the protein digestion and absorption pathway is mainly involved in the regulation of multiple amino acid transport proteins. The activation of cell signaling pathways is closely related to protein hydrolysis and pro-apoptotic processes, while the activation of protein digestion and absorption signaling pathways is mainly related to the levels of various amino acid transport proteins (33). TAM and DOX can cause mitochondrial damage and thus induce apoptosis in breast cancer cells. si-FoxO3a can impair this effect, as when Gln is transported into the cell via SLC38A2, it inhibits the levels of FoxO3a, research indicates that reduced FoxO3a expression leads to excessive glutamine consumption by activated T cells, promoting the tricarboxylic acid cycle and activating mTOR signaling to influence transport processes (34). Downregulating ASNS expression inhibits asparagine synthesis and its downstream mTOR pathway to suppress TNBC progression, while suppression of the mTOR signaling pathway affects FoxO3a levels (35); therefore, si-FoxO3a also affects ASNS expression by regulating the metabolism of various amino acids. Furthermore, it may directly affect the levels of ZYX and TPBG, and indirectly affects the levels of Wnt signaling, by regulating mTOR (36). This indicates a close relationship between FoxO3a and the protein digestion and absorption signaling pathway. TPBG, SLC38A2, ASNS and ZYX are associated with protein digestion and absorption signaling pathways, hence these proteins were selected for validation.

Fig. 10 shows a hypothetical model by which the aforementioned DEPs may participate in the apoptosis process of breast cancer cells. The effect of FoxO3a on SLC38A2 and TPBG requires further experimental validation. TPBG is a transmembrane protein highly expressed mainly in trophoblast and cancer cells (37). It promotes pancreatic cancer cell metastasis through the Wnt signaling pathway, affecting the Wnt downstream protein signaling cascade, causing increased cancer cell migration and reducing apoptosis (38). It also induces lung cancer cell invasion and epithelial-mesenchymal transition by inhibiting the levels of microRNA-15b present (39). The ectopic expression of TPBG markedly promotes the migration and invasive ability of two TNBC lines (40). Studies have demonstrated that TPBG is a therapeutic target for several anticancer drugs currently in clinical development, mainly because of its high expression in tumors and low expression in normal tissues (41,42).

Tumor cells usually take up large quantities of amino acids from the extracellular environment to sustain proliferation and metastasis. Therefore, the upregulation of certain amino acid transporter proteins to obtain large amounts of amino acids acts as an important source of energy for tumor cells (43). The SLC family of proteins contains dozens of members that transport different amino acid types (44). The membrane transporter protein SLC38A2 is mainly responsible for the transport of neutral amino acids, such as Gln (33), and is involved in a range of energy metabolism processes. Therefore, the upregulation of SLC38A2 may help maintain enlarged cell volume to sustain proliferation, thus reducing cell apoptosis. Meanwhile, increased SLC38A2 expression promotes glutamine-dependent cell proliferation and is associated with low survival and resistance to TAM in patients with TNBC (45,46).

Additional studies have demonstrated that the development of drugs targeting SLC38A2 may be of value in some hormone-resistant breast cancers (45,47), demonstrating the importance of its role in future clinical applications. ASNS uses glutamate to provide a nitrogen source to enable aspartic acid to synthesize asparagine (48), and studies have demonstrated that its high expression promotes breast cancer metastasis and colorectal cancer progression (49,50). The downregulation of ASNS inhibits the induction of cell cycle arrest and suppresses cell proliferation (51). With this, its expression levels are associated with that of apoptosis, thus harboring the potential to serve as a prognostic marker for breast cancer (52). ASNS inhibition is essential for targeting asparagine metabolism in cancer (53). Previous studies have demonstrated that elevated asparagine levels catalyzed by ASNS are key for breast cancer metastasis (53,54). Inhibition of the Gln-associated pathway does not reduce the viability of all cancer cell lines, even in Gln-dependent TNBC cell lines (55). Therefore, the low expression of ASNS in si-FoxO3a MDA-MB-231 cells may be due to the substitution of other amino acids for Gln, which serve a role in maintaining the growth of breast cancer cells, resulting in reduced levels of ASNS. This is a hypothesis; therefore, further verification is ultimately required.

ZYX is mainly responsible for the interaction between cells and the extracellular matrix and is involved in the organization and regeneration of the cytoskeleton. It is also involved in in the regulation of adhesion-mediated extracellular matrix signaling (56) to influence the downstream pathways related to cell migration, invasion and apoptosis. ZYX functions not only as an oncogenic protein, but also as an antitumor protein in carcinogenesis (57). On one hand, ZYX promotes the progression of hepatocellular carcinoma by activating the AKT/mTOR signaling pathway (58). ZYX acts as an inhibitor of the growth of colorectal cancer cells and is associated with the levels of p53 (59). Therefore, its role in different types of breast cancer warrants further investigation (60).

It is important to acknowledge the limitations of the present study, as rescue experiments could not be performed due to particular constraints, and only two cell lines were available for experimentation. Additionally, due to a lack of *in vivo* experiments to differentially validate the relationship between the proteins, further exploration is needed to achieve this in the future. Further limitations that should also be noted include the need for verification of the association between FoxO3a and proteins such as SLC38A2 and TPBG. This requires more exploration in future studies. In addition, the proteomics analysis section of the present study was performed by an external service provider. The P-values reported were not corrected, and the lack of multiple testing correction may have resulted in a higher false positive rate.

Breast cancer development involves numerous proteins and signaling molecules, and the results of the present study indicate DEPs after knockdown of FoxO3a are involved in the amino acid transport pathway and mainly serve a role in the protein digestion and absorption signaling pathway (Fig. 10). In conclusion, knocking down FoxO3a inhibits drug-induced

apoptosis in breast cancer cells and alters expression levels of proteins in the protein digestion and absorption signaling pathways.

Acknowledgements

Not applicable.

Funding

Financial support was received for the research and/or publication of the present article. Funding was received from the Natural Science Project of Jilin Provincial Department of Science and Technology (grant no. YDZJ202401085ZYTS), the Jilin Provincial Department of Education Science and Technology Research Project (grant no. JJKH20220460KJ), the Mekong College Student Scientific Research and Innovation Fund Program (grant no. 2023JYMKZ001), and the Jilin Province College Student Innovation and Entrepreneurship Project (grant no. S202413706001).

Availability of data and materials

The data generated in the present study may be found in ProteomeXchange via the iProX partner repository under accession number PXD068299 or at the following URL: https://proteomecentral.proteomexchange.org/cgi/GetDataset?ID=PXD068299.

Authors' contributions

LS and ZW wrote the manuscript, and designed and performed the experiments. YL, JL, HT and XS performed the experiments. CH, YZ, LC and SC analyzed the data. SC was involved in the conception and design of the study. LS and ZW confirm the authenticity of all the raw data. All authors reviewed the results, and read and approved the final version of the manuscript.

Ethics approval and consent to participate

Not applicable.

Patient consent for publication

Not applicable.

Competing interests

The authors declare that they have no competing interests.

References

1. Katsura C, Ogunmwonyi I, Kankam HK and Saha S: Breast cancer: Presentation, investigation and management. Br J Hosp Med (Lond) 83: 1-7, 2022.
2. Avti PK, Singh J, Dahiya D and Khanduja KL: Dual functionality of pyrimidine and flavone in targeting genomic variants of EGFR and ER receptors to influence the differential survival rates in breast cancer patients. Integr Biol (Camb) 15: zyad014, 2023.
3. Fortin J, Leblanc M, Elgbeili G, Cordova MJ, Marin MF and Brunet A: The mental health impacts of receiving a breast cancer diagnosis: A meta-analysis. Br J Cancer 125: 1582-1592, 2021.
4. Ye F, Dewanjee S, Li Y, Jha NK, Chen ZS, Kumar A, Vishakha, Behl T, Jha SK and Tang H: Advancements in clinical aspects of targeted therapy and immunotherapy in breast cancer. Mol Cancer 22: 105, 2023.
5. Castellote-Huguet P, Ruiz-Espana S, Galan-Auge C, Santabarbara JM, Maceira AM and Moratal D: Breast cancer diagnosis using texture and shape features in MRI. Annu Int Conf IEEE Eng Med Biol Soc 2023: 1-4, 2023.
6. Nunnery SE and Mayer IA: Targeting the PI3K/AKT/mTOR pathway in hormone-positive breast cancer. Drugs 80: 1685-1697, 2020.
7. Kotsopoulos J, Gronwald J, Huzarski T, Aeilts A, Armel SR, Karlan B, Singer CF, Eisen A, Tung N, Olopade O, *et al*: Tamoxifen and the risk of breast cancer in women with a BRCA1 or BRCA2 mutation. Breast Cancer Res Treat 201: 257-264, 2023.
8. Masci D, Naro C, Puxeddu M, Urbani A, Sette C, La Regina G and Silvestri R: Recent advances in drug discovery for triple-negative breast cancer treatment. Molecules 28: 7513, 2023.
9. Xu C, Feng Q, Yang H, Wang G, Huang L, Bai Q, Zhang C, Wang Y, Chen Y, Cheng Q, *et al*: A light-triggered mesenchymal stem cell delivery system for photoacoustic imaging and chemo-photothermal therapy of triple negative breast cancer. Adv Sci (Weinh) 5: 1800382, 2018.
10. Hwang KT, Kim J, Jung J, Chang JH, Chai YJ, Oh SW, Oh S, Kim YA, Park SB and Hwang KR: Impact of breast cancer subtypes on prognosis of women with operable invasive breast cancer: A population-based study using SEER database. Clin Cancer Res 25: 1970-1979, 2019.
11. Al-Azhri J, Zhang Y, Bshara W, Zirpoli G, McCann SE, Khoury T, Morrison CD, Edge SB, Ambrosone CB and Yao S: Tumor expression of vitamin D receptor and breast cancer histopathological characteristics and prognosis. Clin Cancer Res 23: 97-103, 2017.
12. Sun Z, Zhou D, Yang J and Zhang D: Doxorubicin promotes breast cancer cell migration and invasion via DCAF13. FEBS Open Bio 12: 221-230, 2022.
13. Jiang D, Qiu T, Peng J, Li S, Tala, Ren W, Yang C, Wen Y, Chen CH, Sun J, *et al*: YB-1 is a positive regulator of KLF5 transcription factor in basal-like breast cancer. Cell Death Differ 29: 1283-1295, 2022.
14. Katzenellenbogen BS, Guillen VS and Katzenellenbogen JA: Targeting the oncogenic transcription factor FOXM1 to improve outcomes in all subtypes of breast cancer. Breast Cancer Res 25: 76, 2023.
15. Francois M, Donovan P and Fontaine F: Modulating transcription factor activity: Interfering with protein-protein interaction networks. Semin Cell Dev Biol 99: 12-19, 2020.
16. Liu TT, Yang H, Zhuo FF, Yang Z, Zhao MM, Guo Q, Liu Y, Liu D, Zeng KW and Tu PF: Atypical E3 ligase ZFP91 promotes small-molecule-induced E2F2 transcription factor degradation for cancer therapy. EBioMedicine 86: 104353, 2022.
17. Pang X, Zhou Z, Yu Z, Han L, Lin Z, Ao X, Liu C, He Y, Ponnusamy M, Li P and Wang J: Foxo3a-dependent miR-633 regulates chemotherapeutic sensitivity in gastric cancer by targeting Fas-associated death domain. RNA Biol 16: 233-248, 2019.
18. Meng XY, Wang KJ, Ye SZ, Chen JF, Chen ZY, Zhang ZY, Yin WQ, Jia XL, Li Y, Yu R and Ma Q: Sinularin stabilizes FOXO3 protein to trigger prostate cancer cell intrinsic apoptosis. Biochem Pharmacol 220: 116011, 2024.
19. Khoshinani HM, Afshar S, Pashaki AS, Mahdavinezhad A, Nikzad S, Najafi R, Amini R, Gholami MH, Khoshghadam A and Saidijam M: Involvement of miR-155/FOXO3a and miR-222/PTEN in acquired radioresistance of colorectal cancer cell line. Jpn J Radiol 35: 664-672, 2017.
20. Wolfe AR, Debeb BG, Lacerda L, Larson R, Bambhroliya A, Huang X, Bertucci F, Finetti P, Birnbaum D, Van Laere S, *et al*: Simvastatin prevents triple-negative breast cancer metastasis in pre-clinical models through regulation of FOXO3a. Breast Cancer Res Treat 154: 495-508, 2015.
21. Chen S, Li YQ, Yin XZ, Li SZ, Zhu YL, Fan YY, Li WJ, Cui YL, Zhao J, Li X, *et al*: Recombinant adenoviruses expressing apoptin suppress the growth of MCF-7 breast cancer cells and affect cell autophagy. Oncol Rep 41: 2818-2832, 2019.
22. Kang BG, Shende M, Inci G, Park SH, Jung JS, Kim SB, Kim JH, Mo YW, Seo JH, Feng JH, *et al*: Combination of metformin/efavirenz/fluoxetine exhibits profound anticancer activity via a cancer cell-specific ROS amplification. Cancer Biol Ther 24: 20-32, 2023.
23. Schmittgen TD and Livak KJ: Analyzing real-time PCR data by the comparative C(T) method. Nat Protoc 3: 1101-1108, 2008.
24. Khan MA, Sadaf, Ahmad I, Aloliqi AA, Eisa AA, Najm MZ, Habib M, Mustafa S, Massey S, Malik Z, *et al*: FOXO3 gene hypermethylation and its marked downregulation in breast cancer cases: A study on female patients. Front Oncol 12: 1078051, 2022.

25. Yang L, Zhang Y, Zhang Y, Xu Y, Li Y, Xie Z, Wang H, Lin Y, Lin Q, Gong T, *et al*: Live macrophage-delivered doxorubicin-loaded liposomes effectively treat triple-negative breast cancer. ACS Nano 16: 9799-9809, 2022.
26. Ansari L, Shiehzadeh F, Taherzadeh Z, Nikoofal-Sahlabadi S, Momtazi-Borojeni AA, Sahebkar A and Eslami S: The most prevalent side effects of pegylated liposomal doxorubicin monotherapy in women with metastatic breast cancer: A systematic review of clinical trials. Cancer Gene Ther 24: 189-193, 2017.
27. Wei Y, Guo Y, Zhou J, Dai K, Xu Q and Jin X: Nicotinamide overcomes doxorubicin resistance of breast cancer cells through deregulating SIRT1/Akt pathway. Anticancer Agents Med Chem 19: 687-696, 2019.
28. Sun L, Liu J, Bao D, Hu C, Zhao Y and Chen S: Progress in the study of FOXO3a interacting with microRNA to regulate tumourigenesis development. Front Oncol 13: 1293968, 2023.
29. Chen YF, Pandey S, Day CH, Chen YF, Jiang AZ, Ho TJ, Chen RJ, Padma VV, Kuo WW and Huang CY: Synergistic effect of HIF-1α and FoxO3a trigger cardiomyocyte apoptosis under hyperglycemic ischemia condition. J Cell Physiol 233: 3660-3671, 2018.
30. Yadav RK, Chauhan AS, Zhuang L and Gan B: FoxO transcription factors in cancer metabolism. Semin Cancer Biol 50: 65-76, 2018.
31. Liu H, Yin J, Wang H, Jiang G, Deng M, Zhang G, Bu X, Cai S, Du J and He Z: FOXO3a modulates WNT/β-catenin signaling and suppresses epithelial-to-mesenchymal transition in prostate cancer cells. Cell Signal 27: 510-518, 2015.
32. Li H, Tang X, Sun Z, Qu Z and Zou X: Integrating bioinformatics and experimental models to investigate the mechanism of the chelidonine-induced mitotic catastrophe via the AKT/FOXO3/FOXM1 axis in breast cancer cells. Biomol Biomed 24: 560-574, 2024.
33. Gauthier-Coles G, Bröer A, McLeod MD, George AJ, Hannan RD and Bröer S: Identification and characterization of a novel SNAT2 (SLC38A2) inhibitor reveals synergy with glucose transport inhibition in cancer cells. Front Pharmacol 13: 963066, 2022.
34. Petry ÉR, Dresch DF, Carvalho C, Medeiros PC, Rosa TG, de Oliveira CM, Martins LAM, Guma FCR, Marroni NP and Wannmacher CMD: Oral glutamine supplementation relieves muscle loss in immobilized rats, altering p38MAPK and FOXO3a signaling pathways. Nutrition 118: 112273, 2024.
35. Yuan Q, Wang Q, Li J, Yin L, Liu S, Zu X and Shen Y: CCT196969 inhibits TNBC by targeting the HDAC5/RXRA/ASNS axis to down-regulate asparagine synthesis. J Exp Clin Cancer Res 44: 231, 2025.
36. Zhao X, Lai H, Li G, Qin Y, Chen R, Labrie M, Stommel JM, Mills GB, Ma D, Gao Q and Fang Y: Rictor orchestrates β-catenin/FOXO balance by maintaining redox homeostasis during development of ovarian cancer. Oncogene 44: 1820-1832, 2025.
37. Park S, Yoo JE, Yeon GB, Kim JH, Lee JS, Choi SK, Hwang YG, Park CW, Cho MS, Kim J, *et al*: Trophoblast glycoprotein is a new candidate gene for Parkinson's disease. NPJ Parkinsons Dis 7: 110, 2021.
38. He P, Jiang S, Ma M, Wang Y, Li R, Fang F, Tian G and Zhang Z: Trophoblast glycoprotein promotes pancreatic ductal adenocarcinoma cell metastasis through Wnt/planar cell polarity signaling. Mol Med Rep 12: 503-509, 2015.
39. Su H, Yu S, Sun F, Lin D, Liu P and Zhao L: LINC00342 induces metastasis of lung adenocarcinoma by targeting miR-15b/TPBG. Acta Biochim Pol 69: 291-297, 2022.
40. Ye F, Liang Y, Wang Y, Yang RL, Luo D, Li Y, Jin Y, Han D, Chen B, Zhao W, *et al*: Cancer-associated fibroblasts facilitate breast cancer progression through exosomal circTBPL1-mediated intercellular communication. Cell Death Dis 14: 471, 2023.
41. Hu G, Leal M, Lin Q, Affolter T, Sapra P, Bates B and Damelin M: Phenotype of TPBG gene replacement in the mouse and impact on the pharmacokinetics of an antibody-drug conjugate. Mol Pharm 12: 1730-1737, 2015.
42. Stern PL, Brazzatti J, Sawan S and McGinn OJ: Understanding and exploiting 5T4 oncofoetal glycoprotein expression. Semin Cancer Biol 29: 13-20, 2014.
43. Kandasamy P, Zlobec I, Nydegger DT, Pujol-Giménez J, Bhardwaj R, Shirasawa S, Tsunoda T and Hediger MA: Oncogenic KRAS mutations enhance amino acid uptake by colorectal cancer cells via the hippo signaling effector YAP1. Mol Oncol 15: 2782-2800, 2021.
44. Kandasamy P, Gyimesi G, Kanai Y and Hediger MA: Amino acid transporters revisited: New views in health and disease. Trends Biochem Sci 43: 752-789, 2018.
45. Morotti M, Zois CE, El-Ansari R, Craze ML, Rakha EA, Fan SJ, Valli A, Haider S, Goberdhan DCI, Green AR and Harris AL: Increased expression of glutamine transporter SNAT2/SLC38A2 promotes glutamine dependence and oxidative stress resistance, and is associated with worse prognosis in triple-negative breast cancer. Br J Cancer 124: 494-505, 2021.
46. Morotti M, Bridges E, Valli A, Choudhry H, Sheldon H, Wigfield S, Gray N, Zois CE, Grimm F, Jones D, *et al*: Hypoxia-induced switch in SNAT2/SLC38A2 regulation generates endocrine resistance in breast cancer. Proc Natl Acad Sci USA 116: 12452-12461, 2019.
47. Stretton C, Lipina C, Hyde R, Cwiklinski E, Hoffmann TM, Taylor PM and Hundal HS: CDK7 is a component of the integrated stress response regulating SNAT2 (SLC38A2)/System A adaptation in response to cellular amino acid deprivation. Biochim Biophys Acta Mol Cell Res 1866: 978-991, 2019.
48. Shen Y, Li M, Xiong Y, Gui S, Bai J, Zhang Y and Li C: Proteomics analysis identified ASNS as a novel biomarker for predicting recurrence of skull base chordoma. Front Oncol 11: 698497, 2021.
49. Du F, Chen J, Liu H, Cai Y, Cao T, Han W, Yi X, Qian M, Tian D, Nie Y, *et al*: SOX12 promotes colorectal cancer cell proliferation and metastasis by regulating asparagine synthesis. Cell Death Dis 10: 239, 2019.
50. Knott SRV, Wagenblast E, Khan S, Kim SY, Soto M, Wagner M, Turgeon MO, Fish L, Erard N, Gable AL, *et al*: Asparagine bioavailability governs metastasis in a model of breast cancer. Nature 554: 378-381, 2018.
51. Yang H, He X, Zheng Y, Feng W, Xia X, Yu X and Lin Z: Down-regulation of asparagine synthetase induces cell cycle arrest and inhibits cell proliferation of breast cancer. Chem Biol Drug Des 84: 578-584, 2014.
52. Qin C, Yang X and Zhan Z: High expression of asparagine synthetase is associated with poor prognosis of breast cancer in Chinese population. Cancer Biother Radiopharm 35: 581-585, 2020.
53. Nishikawa G, Kawada K, Hanada K, Maekawa H, Itatani Y, Miyoshi H, Taketo MM and Obama K: Targeting asparagine synthetase in tumorgenicity using patient-derived tumor-initiating cells. Cells 11: 3273, 2022.
54. Chen W, Qin Y, Qiao L, Liu X, Gao C, Li TR, Luo Y, Li D, Yan H, Han L, *et al*: FAM50A drives breast cancer brain metastasis through interaction with C9ORF78 to enhance L-asparagine production. Sci Adv 11: eadt3075, 2025.
55. Reis LMD, Adamoski D, Souza RO, Ascenção CF, de Oliveira KR, Corrêa-da-Silva F, de Sá Patroni FM, Dias MM, Consonni SR, de Moraes-Vieira PMM, *et al*: Dual inhibition of glutaminase and carnitine palmitoyltransferase decreases growth and migration of glutaminase inhibition-resistant triple-negative breast cancer cells. J Biol Chem 294: 9342-9357, 2019.
56. Partynska A, Gomulkiewicz A, Dziegiel P and Podhorska-Okolow M: The role of zyxin in carcinogenesis. Anticancer Res 40: 5981-5988, 2020.
57. Kotb A, Hyndman ME and Patel TR: The role of zyxin in regulation of malignancies. Heliyon 4: e00695, 2018.
58. Cai T, Bai J, Tan P, Huang Z, Liu C, Wu Z, Cheng Y, Li T, Chen Y, Ruan J, *et al*: Zyxin promotes hepatocellular carcinoma progression via the activation of AKT/mTOR signaling pathway. Oncol Res 31: 805-817, 2023.
59. Mohammadi H, Shakiba E, Rostampour R, Bahremand K, Goodarzi MT, Bashiri H, Ghobadi KN and Asadi S: Down expression of zyxin is associated with down expression of p53 in colorectal cancer. Int J Mol Cell Med 14: 461-471, 2025.
60. Ma B, Cheng H, Gao R, Mu C, Chen L, Wu S, Chen Q and Zhu Y: Zyxin-Siah2-Lats2 axis mediates cooperation between Hippo and TGF-β signalling pathways. Nat Commun 7: 11123, 2016.